Structural modeling of the metastable supercooled LiCl aqueous solution using the Reverse Monte Carlo (RMC) simulation

M. HABCHI[a,b,*], M. ZIANE[c], S.M. MESLI[a,b], A. DEROUICHE[c], F. BENZOUINE[c] M. KOTBI[d].
[a]Ecole Préparatoire en Sciences et Techniques, BP 165RP, Bel Horizon, 13000 Tlemcen, Algeria
[b]ISP group, NMSE division, URMER, Abou Bekr Belkaid University of Tlemcen, Algeria
[c]LPPPC, Physics Department, Sciences Faculty Ben Msik P.O. 7955, Casablanca, Morocco
[d]Department of Physics, LPT, Abou Bekr Belkaid University, BP 119 Tlemcen, Algeria

A 3-dimensional atomic configuration has been created using the Reverse Monte Carlo (RMC) methods in conjunction with the neutron scattering results to model the LiCl aqueous solution (R=6) at the metastable supercooled liquid state (T=162 k). The structural characterization of this state is carried out through the pair distribution functions (PDF) and the numbers of coordination computed from the atomic network. Comparison between the coordination numbers of the three thermodynamic states; liquid, supercooled liquid and glass, shows that the dipole interactions in the restructuring of the hydrogen bonds from the liquid to the glassy state, and the chlorine-water correlations in the hydration shells of chlorine are the causes of the anomalies shown in the partial correlation functions for the supercooled liquid state.

1. Introduction

The electrolytic aqueous solutions are of great importance in electrochemistry and physicochemistry of materials, they are present in our natural and industrial environment, in our food and medicines, in our blood and sweat. Electrolytes play a very important role in our organism, they ensure proper operation. Consequently, they are subject to several experimental and theoretical researches. The aqueous LiCl is one of the most studied solutions by many researchers; they possess the property of forming a glass through a metastable supercooled liquid state when the temperature decreases [1-6].

Many properties of aqueous electrolyte solutions are due to the hydrogen bridge between molecules of water, resulting from orientations and interactions of water molecules and from the other interactions between water-ion and ion-ion, under influence of the salt concentration [2,3,7-19]. The understanding of the thermodynamic states of liquid and glass is, in our view, advanced enough compared to the unavoidable intermediate metastable state. Several persuasive theoretical and experimental studies have been proposed over the last decades to describe and explain the behavior of this state. The purpose of this article is to add another piece in the puzzle of understanding anomalies of water and aqueous electrolytes by performing the first Reverse Monte Carlo (RMC) modeling of the LiCl6H$_2$O at the supercooled state (162k). The aim of this work is to extend and complement previous works by displaying all of pair distribution functions for the supercooled state and computing the numbers and the average positions of coordination between each pair atoms for the three thermodynamic states in order to make a meaningful comparison.

In the framework of this study we use the RMC method in conjunction with neutron diffraction data [20]. This technique of simulation allows the construction of a 3-dimensional model on the atomic level based on both experimental data and some geometric constraints, on the other hand it completes the experiment by computing the pair distribution functions (PDF) g$_{ij}$(r) between each two components of the studied system. The advantage of this method is to be applied without any specified interatomic and/or intermolecular interactions, it can be also, hybridized by introducing a potential pattern as additional constraint [9,11,21-24}.

Implementation method and details of the simulation performed here are described in Section2. In Section 3 we give obtained results and their discussion. Finally in Section 4, conclusion is drawn.

2. Computational details

The RMC algorithm was described in detail elsewhere [25-29]. Only a brief summary will be given here. The aim of this method is to produce three dimensional structural models of ordered or disordered systems in agreement with the available experimental data within fixed standard deviation. This technique is implemented using the same principle of the metropolis Monte Carlo (MMC) algorithm

[30], but instead of minimizing the potential term, the difference between the computed and the experimental total or partial distribution functions is the quantity to be minimized. When satisfactory agreement between experimental and calculated data sets is obtained, the resulting configuration should be a three-dimensional structure compatible with the experimental data and the detailed structural information such as the number of coordination, the nearest neighbors position and bond angle distribution functions can be calculated from the atomic networks.

The cubic atomic configurations of the chloride lithium in water were generated using RMC simulations of scattering neutron data. Four available experimental partial distribution functions $G_{XX}^{Exp}(r)$, $G_{XH}^{Exp}(r)$, $G_{HH}^{Exp}(r)$ and $G_{Cl\alpha}^{Exp}(r)$ obtained by the neutrons scattering technique from the isotopic substitution are used [2,4-6,8]. Which are expressed by:

$$G_{XX}^{Exp}(r) = 0.685\, g_{OO}(r) + 0.37\, g_{OCl}(r) - 0.085\, g_{OLi}(r) + 0.05\, g_{ClCl}(r) - 0.023\, g_{ClLi}(r) + 0.026\, g_{LiLi}(r) \tag{1}$$

$$G_{XH}^{Exp}(r) = 0.828\, g_{OH}(r) + 0.224\, g_{HCl}(r) - 0.051\, g_{HLi}(r) \tag{2}$$

$$G_{HH}^{Exp}(r) = g_{HH}(r) \tag{3}$$

$$G_{Cl\alpha}^{Exp}(r) = 0.28\, g_{OCl}(r) + 0.624\, g_{HCl}(r) + 0.104\, g_{ClCl}(r) - 0.025\, g_{ClLi}(r) \tag{4}$$

where the subscript X defines all atom species except the hydrogen one, while $Cl\alpha$ represents the correlation between Cl and all the other species.

The initial configuration depends on the type of the simulated materials; when studying ordered samples, atoms are positioned in the average crystallographic positions, and several unit cells are used to produce the simulation box. If studying disordered materials, a random distribution of atoms without unreasonably short inter-atomic distances is generated by using an initial code. In this paper, the atomic configuration is a cubic box of 2880 atoms with periodic boundary conditions, where the oxygen atoms form initially a face-centered cubic lattice and the chlorine and lithium atoms are placed in the interstices. The new configurations are obtained by random choices and moves of atoms under geometric constraints and they are accepted or rejected according the same conditions of MMC algorithm. Simulation parameters are summarized in Tables 1 and 2.

Table 1. Closest approach distances $S_{ij}(\text{Å})$ between atom pairs. $S_{ij}^0(\text{Å})$ are used for initially setting up a disordered hard sphere fluid before introducing the experimental curves in the RMC simulation.

	OO	OH	OCl	OLi	HH	HCl	HLi	ClCl	ClLi	LiLi
$S_{ij}(\text{Å})$	2.0	0.92	2.1	1.75	0.9	1.85	2.1	3.75	2.9	3.2
$S_{ij}^0(\text{Å})$	3.0	0.94	2.8	2.0	1.55	2.25	2.25	4.9	4.8	3.2

Table 2. Number of atoms of each species, the total number of atoms N, the total atomic density ρ, the simulation box length L and the temperature of the LiCl6H$_2$O for the three thermodynamic states

	N_O	N_H	N_{Cl}	N_{Li}	N	ρ (atoms/Å^3)	L (Å)	T (k)
Liquid						0.09394	31.297	300
Supercooled	864	1728	144	144	2880	0.09575	31.0993	162
Glass						0.09599	31.0734	120

3. Results and discussions

3.1 Total correlation functions H(r)

The Partial Correlation Functions (PCF), H(r) equivalent to the Partial Distribution Functions G(r) given by H(r)=G(r)-1, are shown in figures 1 and 2. The first one shows the experimental PCFs and also those computed by RMC for the supercooled liquid state, the difference ΔH between them is also drawn to permit an easy comparison. A good agreement and a clear concordance are highlighted between all of the computed and the experimental results. Consequently, the generated 3-dimensional configurations are compatible with the experimental data and thus allow displaying all of the pair distribution functions.

In Fig. 2 the PCFs for the three thermodynamic states; liquid, supercooled liquid and glass are displayed together with the pair distribution functions of the water molecule at ambient temperature. We observe these functions on a reduced variation range for a better distinction between them. A global view of the four functions (on the total interval) as in previous works does not show a significant difference between the two thermodynamic states of glass and supercooled superimposed [2,3], the only visible distinction is in the liquid state; the absence of structure beyond the short and medium range can be shown.

A deeper and more intentioned observation on a reduced variation range containing only meaningful correlations allows a better distinction between the three states and shows interesting behaviors to discuss and to analyze. An intermediate position for the curve of the supercooled state should be in principle predictable as in $G_{HH}(r)=g_{HH}(r)$

directly measured from experiment, however, according to the curves, this prediction is not permanent. The first peaks for the functions namely $H_{XH}(r)$ and $H_{Cl\alpha}(r)$, is more intense in the supercooled state instead to be between liquid and glass and the ascending order of peaks intensity (liquid/supercooled/glass) is reversed in

the $H_{XH}(r)$ correlations. The interpretation of these behaviors must be made by two important parameters; the first one is the weighting factor of PDFs in the linear combination defining PCFs (see equations 1to 4) and the second one is the number of coordination calculated from PDFs.
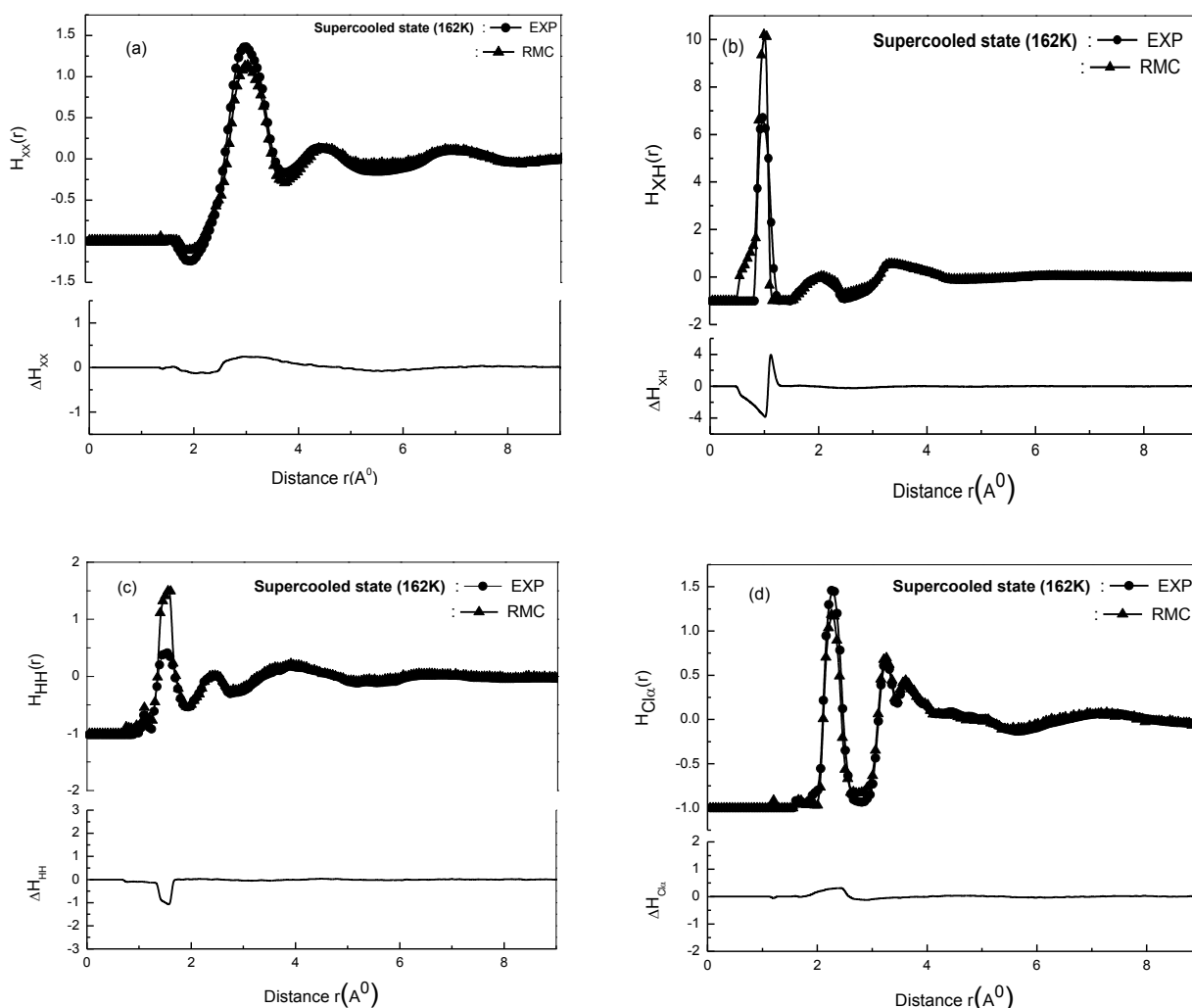
Fig. 1. Experimental and computed Partial Correlation Functions $H_{ij}(r)$ for the supercooled liquid state, ΔH_{ij} is the difference between them

Inspection of the two PCFs $G_{XH}(r)$ (eq. 2) and $G_{Cl\backslash\alpha}(r)$ (eq. 4) stipulates that the correlations of oxygen and chlorine are the more weighted in the linear combinations of these functions. In $G_{XH}(r)$ the dipolar orientations represented by $g_{OH}(r)$ are predominant ($W_{OH}=0.8276$) and the water-ions correlations particularly Cl-water represented by $g_{HCl}(r)$ ($W_{HCl}=0.22365$) are in the second position. In $G_{Cl\backslash\alpha}(r)$ the more important weights are also those of Cl-water correlations; $W_{HCl}=0.642$ and $W_{OCl}=0.28$. The linear combination defining $G_{XX}(r)$ shows the same remarks, where $W_{OO}=0.685$ (water-water correlation) and $W_{OCl}=0.37$(water-Cl). We suggest initially that this instability is due to the competition between molecular dipoles in restructuring and reorganization of hydrogen

bonds on the one hand and to the interactions between chlorine atoms in the hydration shell on the other hand. These suggestions should be verified and confirmed in the next sub-section through the pair distribution functions and the coordination numbers.

3.2. Pair distribution functions

In order to compare efficiently between the coordination numbers and locate the supercooled state in the spectrum of the three thermodynamic states, we have seen fit to use the same range of variations around the coordination peaks for all the pair distribution functions. The structure of a solution will be discussed as usually in terms of the water-water correlations, the structure of the hydration shells represented

by the water-ion correlation, and finally the ion-ion correlations.

3.2.1. Pair distribution functions Water-Water

Before beginning any discussion, it is very important to observe the structure of water molecule in the pure liquid and in the solution. The pair distribution functions between atoms constituting the water molecule

in the solution for the three thermodynamic states together with the pure water are shown in Fig. 3. According to the findings of Fig. 3.b and Fig. 3.c, the structure of the water molecule in the solution is unaltered by ions for both thermodynamic states liquid and glass as reported in previous work [2,3,9]. The same remark is observed for the metastable supercooled liquid, but it is noteworthy that the coordination positions in the solution are slightly offset with respect to the pure water.
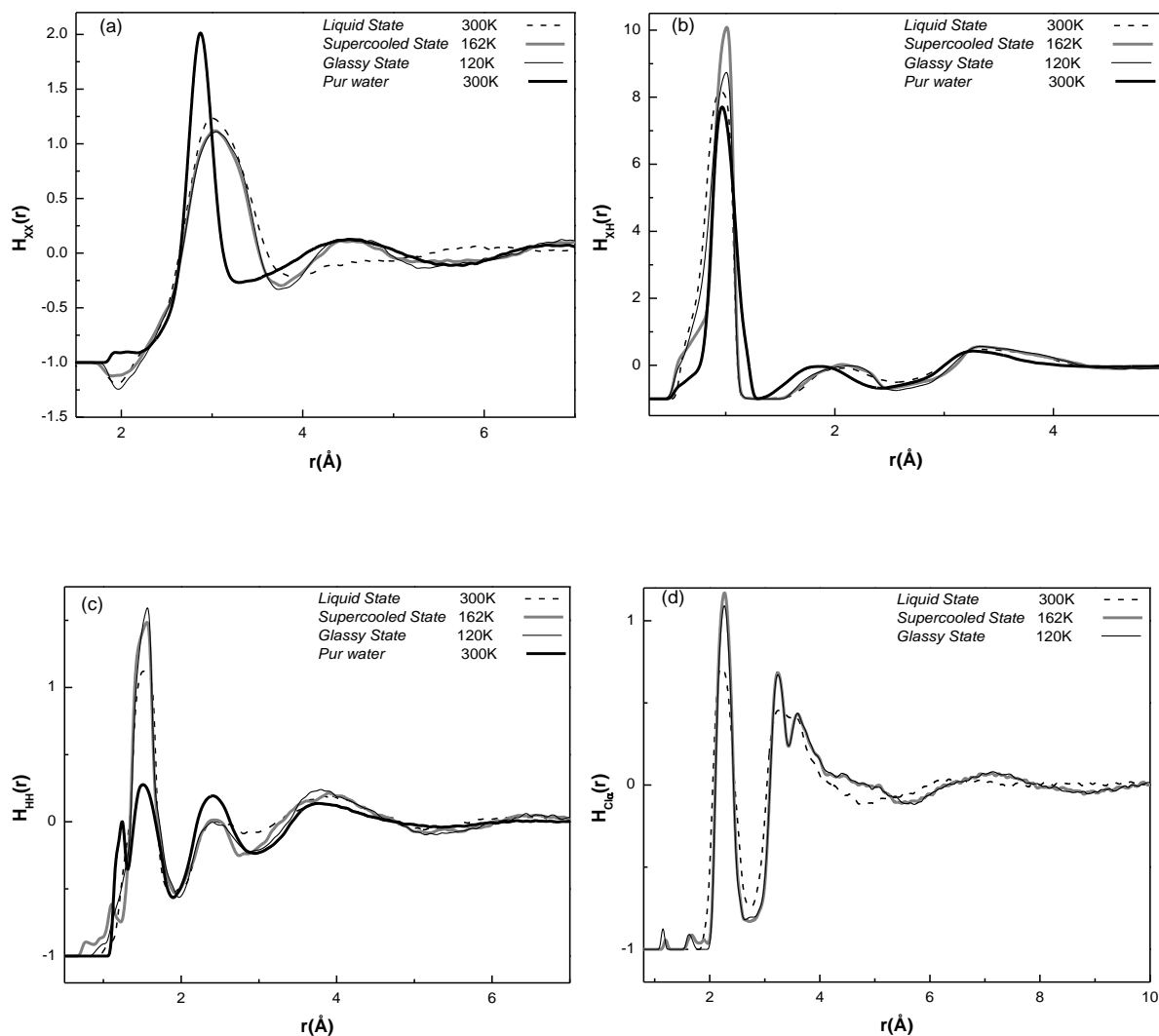
Fig. 2. Partial Correlation Functions $H_{ij}(r)=G_{ij}-1$, where $ij=XX$, XH, HH and $Cl\backslash\alpha$, for the three thermodynamic states together with the intermolecular $h_{kl}(r)=g_{kl}(r)-1$, where $kl=OO$ (a), OH (b) and HH (c) for pure water at room temperatures

The intramolecular correlations of water; O-H and H-H are represented respectively by the first peaks of the pair distribution functions of $g_{OH}(r)$, located at r=0.97Å (Fig. 3.b) and $g_{HH}(r)$ located at r=1.5Å (Fig. 3.c), whereas the competition between dipole moments and their orientations, oxygen network and the arrangement of hydrogen-bonds between molecules of water are observed through the intermolecular correlations O-O, O-H and H-H represented respectively by all peaks of

the $g_{OO}(r)$ (Fig. 3.a) and the 2nd and the 3rd peaks of $g_{OH}(r)$ (Fig. 3.b) and $g_{HH}(r)$ (Fig.3.c). The transition from liquid to glass is explained by the restructuring and the reorganization of hydrogen bonds, the oxygen network is also established at the glassy state. This structure is broken when temperature increases.

The structure of the solution in the supercooled state is closer to the glass than the liquid, this finding is verified by the appearance of a second neighbor intermolecular distance

of O-O at 4.4Å as in the glassy state, this means that the oxygen network begins to be reorganized at the medium range since the supercooled state. The distinction is easily made by comparing the two states through the computed numbers of coordination for the first and the second near-neighbors' peaks located at r = 2.91Å and r=4.4Å, respectively. The coordination number of the second intermolecular correlation is inversely proportional to the temperature (see table 3); we suggest that the supercooled state behaves as an equilibrium state at the medium range, but at the short range (r=2.91Å) the coordination number is proportional to the temperature (see table 3); however, the oxygen network is more structured at short range in going from the glass to the liquid. This behavior is in agreement with that observed in the first peak of $G_{XX}(r)$, where the weight of $g_{OO}(r)$ is the largest one. We suggest that this opposite behavior is due to the correlations O-O and to the Cl-Water with a less effect.

Table 3. intramolecular features for the three thermodynamic states: liquid, supercooled liquid and glass: average positions (Å), coordination numbers and the integration range

		Liquid	Supercooled	Glass
Intramolecular	OH1 (Å)	0.97	0.97	0.97
	(integration range in Å)	(0; 1.25)	(0; 1.25)	(0; 1.25)
	Coordination number n_{OH1}	2.02	2.03	2.02
	HH1 (Å)	1.5	1.5	1.5
	(integration range in Å)	(1.2; 1:9)	(1.2; 1:9)	(1.2; 1.9)
	Coordination number n_{HH1}	1.46	1.56	1.62
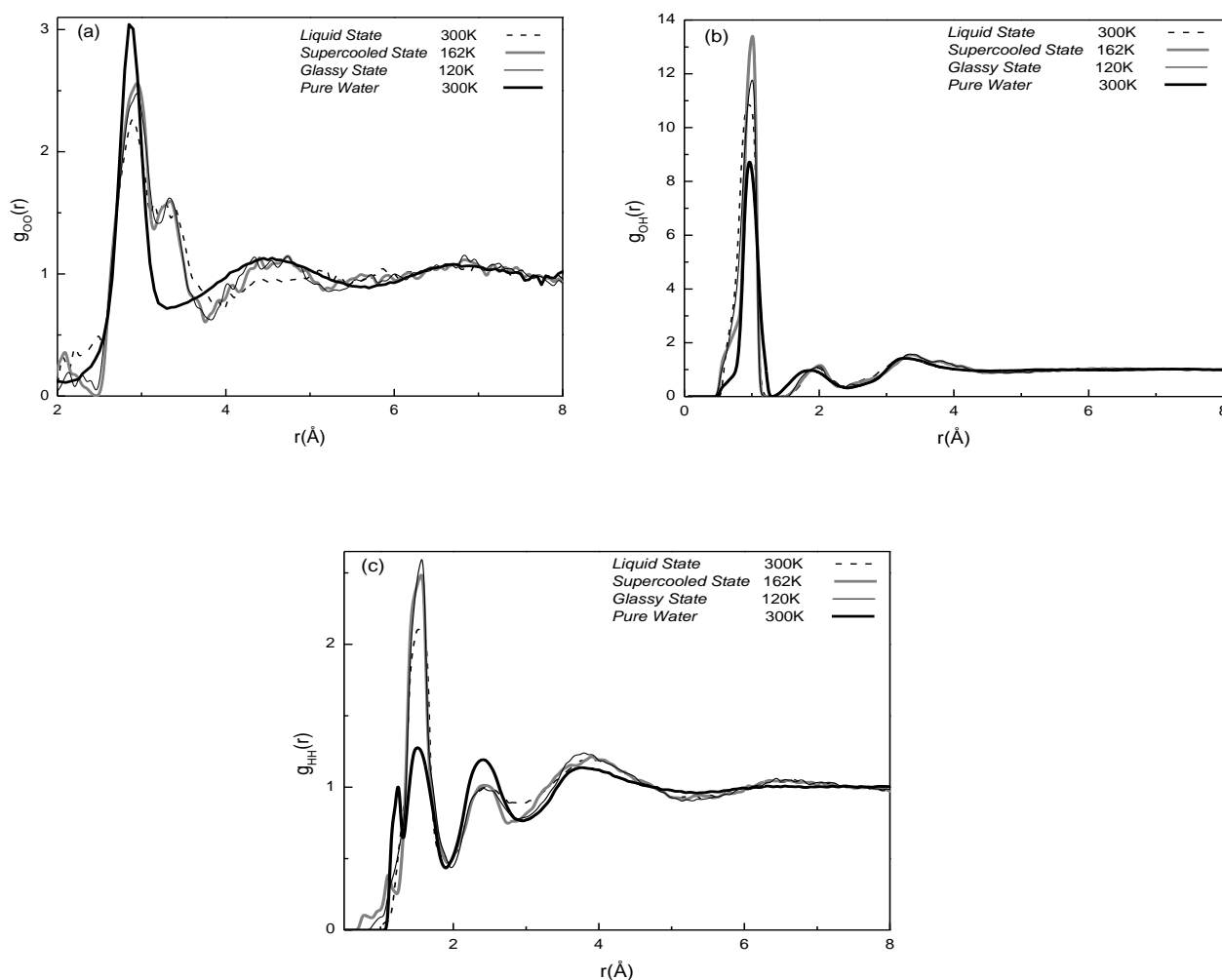
Fig. 3. Pair distribution functions water-water: $g_{OO}(r)$ (a), $g_{OH}(r)$ (b) and $g_{HH}(r)$ (c) at the Glassy, Supercooled Liquid and Liquid states contrasted to the pure water at room temperature.

3.2.2. Pair distribution functions Water-Ion

Discussions on water-ion correlation are closely related to the hydration shells in the neighborhood of cations and anions, which are most frequently elucidated by the number of water molecules around the ions and the way these molecules are oriented. Enumeration of the water molecules is not obtained directly from only one PDF curve; it results from a combination between the number of coordination of one ion versus oxygen and hydrogen atoms, $g_{Oi}(r)$ and $g_{Hi}(r)$.

The structural characteristics of hydration shells, according to several studies [10,12,16], are more reliable for concentrated aqueous solutions, whose the solutes dissolve well in water, as the case of our system. The hydration is due to the polar nature of the water molecule, the negative partial charge of the oxygen atom is attracted by the cation Li^+ and the positive partial charges of hydrogen atoms are repulsed by the same cation [31]; the positively charged cations orient water molecules so that they situate non-bonded oxygen atoms near the cation [13,32-36].
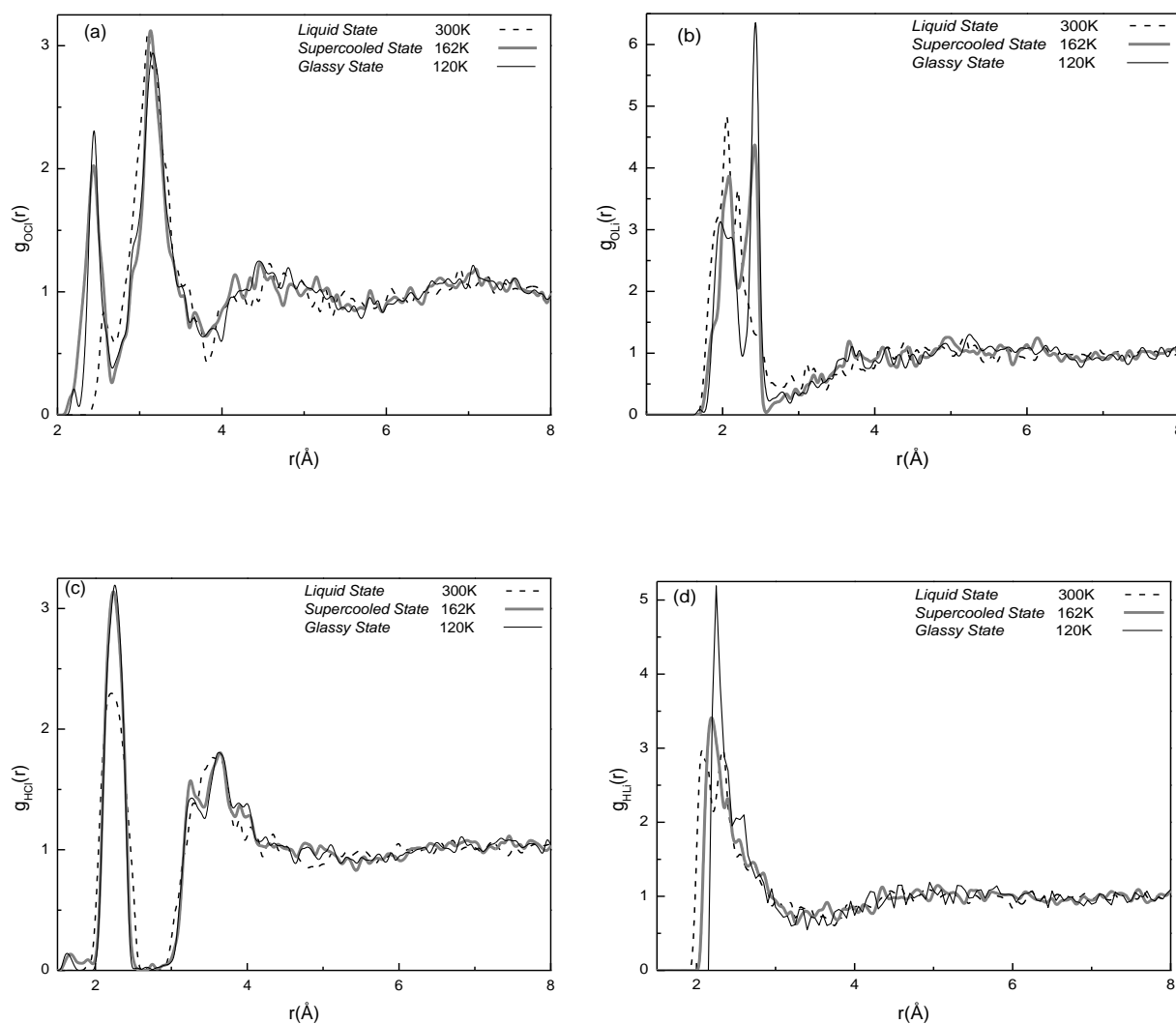
Fig. 4. Pair distribution functions water-Ion: $g_{OCl}(r)$ (a), $g_{OLi}(r)$ (b), $g_{HCl}(r)$ (c) and $g_{HLi}(r)$ (d) at the Glassy, Supercooled Liquid and Liquid states

Hydration shells around the chlorine and the lithium are observed in Fig. 4.a/c and Fig .b/d, respectively. The results show a good agreement with the known findings cited in literature [10,12,16], according to the coordination numbers computed from the Water-Li correlations ($g_{OLi}(r)$ and $g_{HLi}(r)$) the lithium ion is hydrated by 3 to 4 molecules of water. The number of hydrogen first near-neighbors of lithium is around the

double of the oxygen number which are in the same neighborhood near r≈2Å see table 4, this means that these atoms constitute the same molecules of water for the first hydration shell, while the first near-neighbors hydrogen (located at r=2.2Å) and oxygen (located at r=3.1Å) around the chlorine are not in the same neighborhood and thus, they are not in the same molecules of water. A prepeak observed in the $g_{OCl}(r)$ curve (Fig. 4.a) for the supercooled liquid and

the glassy states (almost inexistent in the liquid state) at r=2.2Å can be the effect of oxygen linked to the first hydrogen near-neighbors around chlorine, the number of water molecules at this distance according to the number of hydrogen must be in a rate of 1.5 molecule, and thus this number cannot represent a first hydration shell as known in literature [12,16]. The second hydrogen near-neighbors located at r=3.2Å are in the same neighborhood of the first near-neighboring oxygen i.e. they form the same water molecules defining a hydration shell consisting of about six water molecules. We find that the Li$^+$ hydration shell is well defined and stable compared to the chlorine one. The average distances of the Li-O and Li-H pairs and numbers of coordination (see Fig. 4.b/d and table 4) confirms these findings.

According to the computed intermolecular coordination numbers in order to compare between the

three thermodynamic states, some anomalies are observed for the supercooled state. The concerned correlations are particularly that of water-Cl, we can find that the chlorine-hydrogen coordination number of the supercooled state is the greatest (see table 4). This result is consistent with that observed in the partial correlation functions $G_{XH}(r)$ (Fig. 2.b) and $G_{Cl\backslash\alpha}(r)$ (Fig. 2.d); the first peaks of the supercooled state is more pronounced, where the weighting factor of $g_{HCl}(r)$ is the largest one in the linear combination of $G_{Cl\backslash\alpha}(r)$ (eq. 4) and in $G_{XH}(r)$ (eq. 2) represents the second largest weighting after that of $g_{OH}(r)$. We find that the H-Cl correlations tend to be reinforced out of equilibrium, this finding is justified by the simultaneous reduction of O-Cl correlation number in the supercooled with respect to the liquid state and becomes equal to that of glass (see table 4).

Table 4: intermolecular features for the three thermodynamic states: liquid, supercooled liquid and glass: average positions (Å), coordination numbers and the integration range

		Liquid	Supercooled	Glass
Intermolecular	OH2 (Å)	2	2	2
	(integration range in Å)	(1.25; 2.4)	(1.25; 2.4)	(1.25;2.4)
	Coordination number n_{OH2}	1.45	1.66	1.7
	HH2 (Å)	2.4	2.4	2.4
	(integration range in Å)	(1.9; 2.8)	(1.9; 2.9)	(1.9; 2.9)
	Coordination number n_{HH2}	3.07	3.43	3.48
	OO1 (Å)	2.92	2.91	2.91
	(integration range in Å)	(0; 3.7)	(0; 3.7)	(0; 3.7)
	Coordination number n_{OO1}	6.66	6.43	6.39
	OO2 (Å)		4.4	4.4
	(integration range in Å)		(3.7; 5.3)	(3.7; 5.3)
	Coordination number n_{OO2}		11.95	12.02
	OCl (Å)	3.1	3.1	3.1
	(integration range in Å)	(2.3; 3.7)	(2.3; 3.7)	(2.3; 3.7)
	Coordination number n_{OCl}	6.68	6.3	6.3
	HCl (Å)	2.2	2.2	2.2
	(integration range in Å)	(1.9; 2.6)	(1.9; 2.6)	(1.9; 2.6)
	Coordination number n_{HCl}	3.21	3.35	3.21
	OLi (Å)	2.2	2.2	2.2
	(integration range in Å)	(1.6; 2.5)	(1.6; 2.5)	(1.6; 2.5)
	Coordination number n_{OLi}	3.1	3.32	3.3
	HLi (Å)	2.1	2.1	2.1
	(integration range in Å)	(1.9; 3.25)	(1.9; 3.25)	(1.9; 3.25)
	Coordination number n_{HLi}	7.7	8.03	8.18
	ClLi (Å)		2:92	2:92
	(integration range in Å)		(2.1; 3.2)	(2.1; 3.2)
	Coordination number n_{ClLi}		0.59	0.63

3.2.3. Pair distribution functions Ion-Ion

In the correlations of the same ions, no structure is observed (see Fig. 5.a/c) and the $g_{LiCl}(r)$ shown in Fig. 5.b, is the only function to be discussed in this part. A very sharp, intense peak at r=2.92Å due to Li-Cl contacts. The number of coordination computed around

this peak between 2.1 Å and 3.2 Å is of 0.59 for the supercooled state and 0.63 for the glassy state. This result means that the recombination is possible for both supercooled and glassy thermodynamic states.
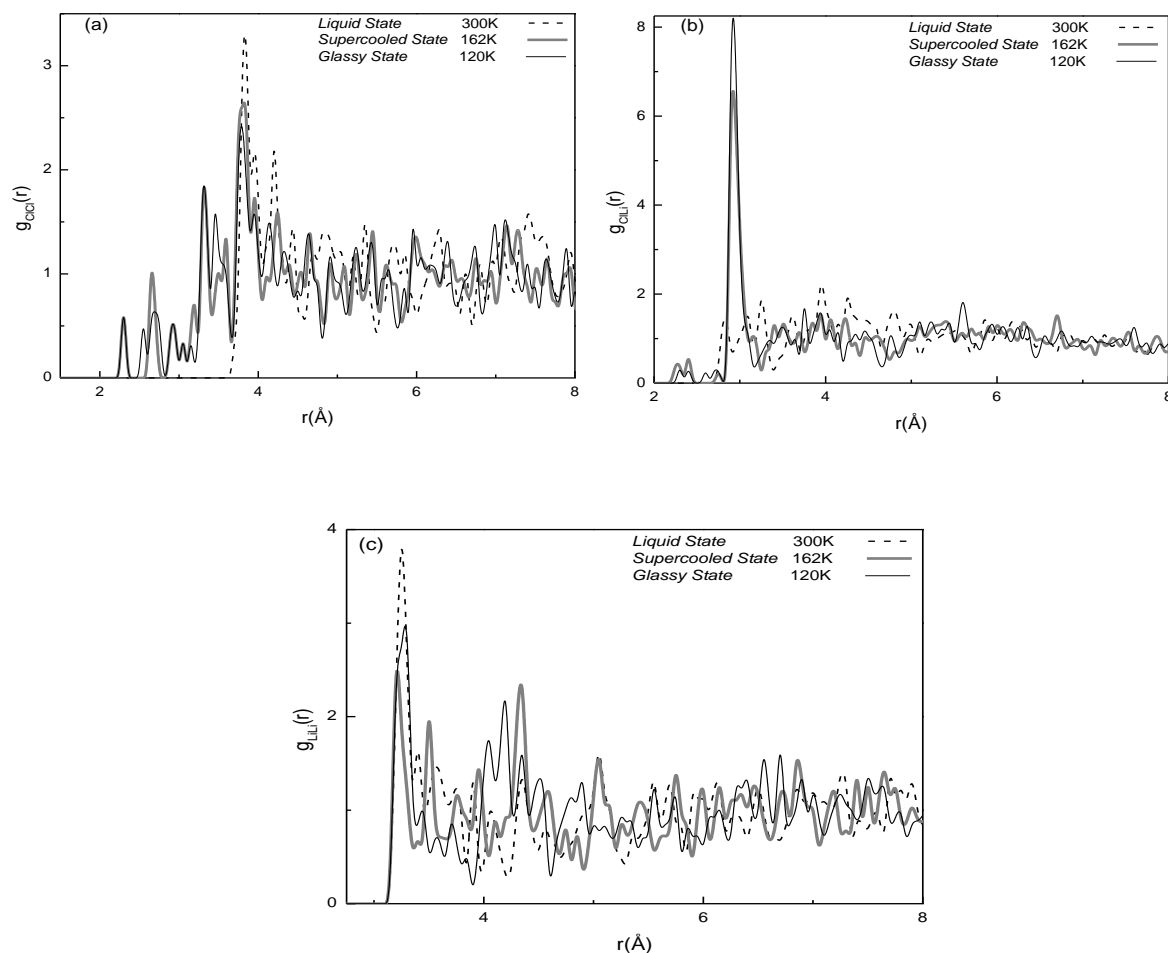
Fig. 5: Pair distribution functions Ion-Ion: $g_{ClCl}(r)$ (a), $g_{ClLi}(r)$ (b) and $g_{LiLi}(r)$ (c) at the Glassy, Supercooled liquid and Liquid states

4. Conclusions

In this paper, we have investigated the structure of the chloride lithium aqueous solutions $LiCl6H_2O$ at the supercooled liquid state by the Reverse Monte Carlo simulation on the basis of available neutron diffraction data. The main peaks of some PCFs for the supercooled state have been found more intense instead to be between the liquid and the glassy states. The inspection of the linear combination of these functions showed that the causes of this behavior are due to the water-water and the chlorine-water correlations in the restructuring of the hydrogen bonds and the hydration shells from the liquid to the glassy state. These findings were confirmed through a meaningful comparison of the calculated numbers of coordination between the three thermodynamic states.

References

[1] K. Winkel, M. Seidl, T. Loerting, L.E. Bove, S. Imberti, V. Molinero, F. Bruni, R. Mancinelli, and M.A. Ricci J. Chem. Phys **134**, 024515 (2011).

[2] B. Prvel, J.F. Jal, J. Dupuy-Philon, A.K. Soper, J. Chem. Phys **103**, 1886 (1995),.

[3] M. Kotbi, H. Xu, Mol. Phys **94**, 373 (1998),.

[4] J.F. Jal, K. Soper, P. Carmona, J. Dupuy, J. Phys: Condens. Matter 3, 551 (1991),.

[5] J. Dupuy-Philon, J.F. Jal, B. Prvel, J. Mol. Liq **64**, 13 (1995),.

[6] A. Aouizerat-Elarby, H. Dez, B. Prevel, J.F. Jal, J. Bert, J. Dupuy-Philon, J. Molec. Liq. **84**, 289 (2000),.

[7] Li. Fei, Yuan. Junsheng, Li. Dongchan, Li. Shenyu, Han. Zhen, J. Molecular Structure **1081**, 38 (2015).

[8] A. Chandra, J. Phys. Chem. B 107, (2003), 3899-3906.

[9] M. Habchi, S. M. Mesli, M. Kotbi, H. Xu, Eur. Phys. J. B **85**, 255 (2012).

[10] Jia-Jia Xu, Hai-Bo Yi, Hui-Ji Li, Yun Chen J. Molecular Physics, 860244 (2013).

[11] M. Kotbi, H. Xu, M. Habchi, Z. Dembahri, Phys. Lett. A **315**, 463 (2003).

[12] I. Harsnyi and L. Pusztai, J. Chem. Phys **137**, 204503 (2012),.

[13] I. Harsnyi, Ph.A. Bopp, A. Vrhovek, L. Pusztai, J. Mol. Liq **158**, 61 (2011).

[14] S. Bouazizi, S. Nasr, J. Molecular Structure **875**, 121 (2008).

[15] S. Bouazizi, S. Nasr, J. Mol. Liq **197**, 77 (2014).

[16] Eva. Pluharova, Henry.E. Fischerb, Philip. E. Masona, and Pavel. Jung-wirth J. Molecular Physics **112**, 1230 (2014).

[17] A. Botti, F. Bruni, S. Imberti, M.A. Ricci, A.K. Soper J. Chem. Phys **120**, 10154 (2004),.

[18] F Bruni, M.A. Ricci, and A.K. Soper J. Chem. Phys **114**, 8056 (2001),.

[19] S. Chowdhuri and A. Chandra J. Chem. Phys **115**, 3732 (2001),.

[20] R.L. Mc Greevy, M.A. Howe, J.D. Wiks,RMCA , A General Purpose Reverse Monte Carlo 3, (1993).

[21] S. M. Mesli, M. Habchi, M. Kotbi, H. Xu. Condens. Matter. Phys. **16**, 1 (2013).

[22] G. Opletal, T. C. Petersen, B. O'Malley, I. K. Snook, D. G. Mc Culloch, I. Yarovsky, Comput. Phys. Commun. **178**, 777 (2008),.

[23] G. Opletal, T. C. Petersen, D. G. Mc Culloch, I. K. Snook, I. Yarovsky, J. Phys. Condens. Matter **17**, 260 (2005).

[24] G. Opletal, T. C. Petersen, B. O'Malley, Snook I.K., D. G. Mc Culloch, N. Marks, I. Yarovsky, Mol. Simul. **28**, 927 (2002).

[25] R.L. Mc Greevy, P. Zetterstrm, Curr. Opin. Solid State Mater. Sci. **7**, 41 (2003).

[26] R.L. Mc Greevy, L. Pusztai, Molec. Simul **1**, 359 (1988).

[27] R.L. Mc Greevy, J. Cond. Matter **13**, R877 (2001).

[28] W.M. Bartczac, J. Kroh, M. Zapalowzki, K. Pernal, Philos. Trans. Roy. Soc. Lond. **359**, 1539 (2009).

[29] Z. Jing-Xiang, L. Hui, Z. Jie, S. Xi-Gui, B. Xiu-Fang, J. Chin. Phys Soc **18**, 1674 (2009).

[30] N. Metropolis, A.W. Rosenbluth, M.N. Rosenbluth, A.H. Teller, E. Teller, J. Chem. Phys. Chem. **21**, 1087 (1953).

[31] S. Cummings, J. E. Enderby, G.W. Neilson, J.R. Newsome, R.A. Howe, W.S. Howells, A.K. Soper, Nature London **87**, 714 (1980),.

[32] K. Ibuki and Ph. A. Bopp, J. Mol. Liq **147**, 56 (2009).

[33] I. Harsnyi, L. Pusztai, J. Chem. Phys **122**, 124512 (2005),.

[34] I. Harsnyi, L. Temleitner, B. Beuneu, L. Pusztai, J. Mol. Liq **165**, 94 (2012),.

[35] H. Ohtaki, T. Radnai, Chem. Rev **93**, 1157 (1993).

[36] A. H. Narten, F. Vaslow, H. A. Levy, J. Chem. Phys **58**, 5017 (1973).

[*]Corresponding author: m.habchi@epst-tlemcen.dz